Carbohydrate Polymers 83 (2011) 1730–1739

Contents lists available at ScienceDirect

Carbohydrate Polymers

journal homepage: www.elsevier.com/locate/carbpol

Highly crystalline chitosan produced by multi-steps acid hydrolysis in the solid-state

Anayancy Osorio-Madrazo[a,b,c,1], Laurent David[a], Stéphane Trombotto[a], Jean-Michel Lucas[a], Carlos Peniche-Covas[b], Alain Domard[a,*]

[a] Laboratoire des Matériaux Polymères et des Biomatériaux, UMR CNRS 5223, Ingénierie des Matériaux Polymères (IMP), Université de Lyon, Université Claude Bernard Lyon 1, Bâtiment ISTIL, 15 Boulevard André Latarjet, F-69622 Villeurbanne Cedex, France
[b] Centro de Biomateriales – Universidad de La Habana, Ave. Universidad s/n, 10600 Ciudad de La Habana, Cuba
[c] Facultad de Química-Farmacia – Universidad Central de Las Villas, Km 5 1/2 Carretera a Camajuaní, 54830 Santa Clara, Cuba

ARTICLE INFO

Article history:
Received 2 July 2010
Received in revised form 12 October 2010
Accepted 19 October 2010
Available online 27 October 2010

Keywords:
Crystalline chitosan
Solid-state hydrolysis
Multi-steps hydrolysis
Crystallinity
Hydrated polymorph
Anhydrous polymorph

ABSTRACT

A multi-steps solid state hydrolysis of chitosan with 3 and 12 M HCl including typical intermediate washings was performed at room temperature. This original treatment induced the processing of highly crystalline materials with polymorphic changes. At each step, a slow decrease of the molecular weight and a plateau in the X-ray crystallinity index (*CrI*) variation was observed with time. *CrI* increased up to 88% with the chain re-crystallization, and the transformation of the hydrated to the anhydrous allomorph. Different factors were at the origin of the plateau of *CrI* observed: (i) the hydrolysis rate decreased after consumption of easily accessible amorphous parts, (ii) crystals of the anhydrous polymorph resulting from the reaction hindered the access of reagents to the remaining amorphous parts. Both mechanisms assumed a decreasing access to reagents: the former during the early stages of hydrolysis, the latter at longer times. The important role played by the multi-steps process with appropriate washings was interpreted and justified. A scheme is proposed to describe the mechanisms involved during hydrolyses.

1. Introduction

Chitosan, a linear natural co-polysaccharide of (1 → 4)-linked-2-acetamido-2-deoxy-β-D-glucan (GlcNAc) and 2-amino-2-deoxy-β-D-glucan (GlcN) is produced from the N-deacetylation of chitin, mainly extracted from crustacean cuticles. When it is soluble in dilute acidic media, it is termed chitosan. If it is obtained by heterogeneous deacetylation, it has a degree of acetylation (*DA*) below 40%, although, a statistic re-acetylation of low *DA* chitosans yields soluble copolymers up to *DA*s of about 70% (Sorlier, Viton, & Domard, 2002; Varum, Ottoy, & Smidsrod, 1994).

In the last decade, numerous works reported on the application of crystalline microfibrils based on natural polymers, termed whiskers, constituted of crystalline slender parallelepiped rods. Composites prepared by casting mixtures of cellulose/chitin whiskers and polymer lattices have shown excellent mechanical properties even at low whisker content due to the formation of a whisker network in the polymer matrix (Angles & Dufresne, 2001; Dubief, Samain, & Dufresne, 1999; Mathew & Dufresne, 2002). Chitosan, which presents the rare property of bioactivity has been poorly studied for nanocomposite filler applications. Crystalline chitosan microfibrils as rigid fillers in composites could be potential for tissue engineering/repair due to its outstanding biological and reinforcing properties.

Almost no work has been published showing the preparation of highly crystalline chitosan with a microfibril morphology. More than two decades ago only one short communication reported about the preparation of a smooth gel of microfibrillated chitosan in water, by homogenization of chitosan flakes (Yokota, 1986). We recently reported on the kinetics of the solid-state hydrolysis of chitosan in concentrated acid (Osorio-Madrazo et al., 2010). The observed increase in crystallinity was related both to the production of anhydrous polymorph, after hydrolysis, and the partial elimination of amorphous regions in the material. In earlier works, the anhydrous polymorph had only been produced by annealing at high temperature (Ogawa, 1991; Ogawa, Hirano, Miyanishi, Yui, & Watanabe, 1984; Saito, Tabeta, & Ogawa, 1987) or displacement of the acid of an acidic complex of chitosan at room temperature and

* Corresponding author.
E-mail address: alain.domard@gmail.com (A. Domard).
[1] Present address: Max Planck Institute of Colloids and Interfaces, Wissenschaftspark Golm, D-14424 Potsdam, Germany.

0144-8617/$ – see front matter © 2010 Elsevier Ltd. All rights reserved.
doi:10.1016/j.carbpol.2010.10.035

Table 1
Characteristics of fully deacetylated chitosans used as starting materials in the multi-steps solid-state acid hydrolysis.

Starting chitosan	*DA* (%, n/n)	Water content (%, w/w)	$M_n/10^5$ (g/mol)	DP_n	I_p	*CrI* (%)
Ch1-D2	0.4	8.12	1.10 ± 0.03	680 ± 2	1.81 ± 0.02	67.1 ± 0.4
Ch1-D2′	0.1	7.73	1.16 ± 0.03	720 ± 2	1.55 ± 0.01	68.5 ± 0.2

high humidity conditions (Okuyama, Noguchi, Hanafusa, Osawa, & Ogawa, 1999). In these cases, the relative proportion of anhydrous or hydrated polymorph was related to parameters like: temperature, the origin of the sample, the molecular weight and *DA* (Ogawa, 1991; Ogawa et al., 1984; Saito et al., 1987).

Our previous studies, restricted to a single step (Osorio-Madrazo et al., 2010) were performed at different HCl concentrations and temperatures. They allowed a better understanding of the hydrolysis kinetics and the concomitant crystallization mechanisms responsible for the formation of the anhydrous allomorph (Osorio-Madrazo et al., 2010). They showed the rapid achievement of a plateau in the evolution of the crystalline ratio with the hydrolysis time. Since, both the reactive (water) and the catalyst (HCl) were used in excess, it seemed that the decrease in the hydrolysis rate and then, the plateau noticed during the kinetics was essentially related to physical phenomena. In this one step process we observed that with the increase in the hydrolysis temperature, crystals produced from the beginning of the reaction started to be destroyed at longer times and did not allow an increase of crystallinity above a critical limit (Osorio-Madrazo et al., 2010). Therefore, in order to reach higher crystalline ratios we preferred to work at low temperature, especially at room temperature. Nevertheless, the increase in *CrI* remained relatively low when obtained from a one-step hydrolysis.

In this work we report on the preparation of the most highly crystalline high molecular weight chitosan obtained up to now by preserving the microfibril morphology of the original material (chitin of arthropod cuticles). To this end, we used a multi-steps process of hydrolysis at room temperature where the material was never dissolved. The relationship between crystalline changes and the plateau reached by *CrI* with the gradual decrease of the hydrolysis rate was better addressed in multi-steps experiments. The present paper focuses on the evolution of the crystalline and macromolecular structures of chitosan by means of a comparative study of the subsequent steps of hydrolysis in the solid-state using different HCl concentrations, and evaluating the important role of the washing conditions between each step.

2. Materials and methods

The initial chitosan, Ch1, produced from shrimp shell chitin, was supplied by Mahtani Chitosan (India, batch no. 2224), with the following molecular characteristics: number-average molecular weight $M_n = 1.48 \pm 0.07 \times 10^5$ g/mol, $DA = 22.7 \pm 0.2\%$, crystallinity index $CrI = 56.7 \pm 0.5\%$, water content $9.5 \pm 0.5\%$ (w/w), and ash content 0.1% (w/w). The processing of the fully deacetylated chitosans Ch1-D2, and Ch1-D2′ both obtained from Ch1 using a heterogeneous deacetylation combined with freeze–pump out–thaw (FPT) cycles (Lamarque, Cretenet, Viton, & Domard, 2005) is described in our previous work (Osorio-Madrazo et al., 2010), and their characteristics are reminded in Table 1.

2.1. Solid-state acid hydrolysis of chitosan with concentrated HCl

Fully deacetylated chitosan flakes were hydrated by stirring in presence of a chosen amount of distilled water. Then, concentrated HCl was added and the mixture shaken. The volume of HCl, V_{HCl}, to be added to obtain a molar ratio of water to glucosamine residue, r_{H_2O}, was calculated from Eq. (1)

$$r_{H_2O} = \frac{V_{HCl} \cdot [(\rho_c - C_{HCl} \cdot M_{HCl})/M_{H_2O}] + (m \cdot w)/M_{H_2O}}{(1 - DA) \cdot (1 - w) \cdot m \cdot [(1 - DA)/M_{GlcN} + DA/M_{GlcNAc}]} \quad (1)$$

where C_{HCl} is the concentration of added HCl (mol L^{-1}); V_{HCl} is the volume of added HCl (L); m is the weight of chitosan (g); w is the water content (weight fraction) of chitosan; ρ_c is the volumic mass of the HCl solution (g L^{-1}) at a concentration C_{HCl}, and M_{GlcN}, M_{GlcNAc}, M_{HCl} and M_{H_2O} are the molecular weights (g mol^{-1}) of glucosamine and N-acetyl-glucosamine residues, HCl and H_2O, respectively.

2.2. Washings and isolation of the hydrolyzed chitosan

Hydrolyzates were placed first in 1.5 M HCl for a few minutes. Then, between the different hydrolysis steps in the multi-steps procedure, the remaining solid was washed according to two different ways. In a first, it was successively poured in 1 M ammonia then, distilled water until neutrality, and finally freeze-dried. In a second, it was only washed with 1.5 M HCl between the different steps. Nevertheless, at the end of the multi-steps procedure, the isolation of the samples consisted in the three washings operated as above and a drying by evaporation.

2.3. Characterization of materials

Molecular weights. Weight- and number-average molecular weights (M_w and M_n) were evaluated by Size-Exclusion Chromatography (SEC). Chitosan solutions at 0.1% (w/v) were prepared in a AcOH (0.2 M)/$AcONH_4$ (0.15 M) pH = 4.5 buffer, used as eluent, then, filtered through 0.22 μm pore size membranes (Millipore). The chromatographic equipment was composed of an IsoChrom LC pump (Spectra-Physics) connected to a Protein Pack 200 SW (WATERS) column and a TSK gel G6000 PW_{XL}. A multi-angle laser light scattering (MALLS) detector DAWN DSP (Wyatt) operating at 632.8 nm was coupled on line to a WATERS 410 differential refractometer. Depending on *DA* (Schatz, Viton, Delair, Pichot, & Domard, 2003), the refractive index increment d*n*/d*c* ranged from 0.183 to 0.198 $cm^3\ g^{-1}$.

Wide-angle X-ray scattering. Chitosan pellets of 1 mm thickness were analyzed by X-ray diffraction for estimating *CrI*. Wide-angle X-ray scattering (WAXS) patterns were recorded in reflection mode with a SIEMENS D 500 diffractometer operating at 35 kV and 30 mA with the Cu Kα radiation. Chitosan tablets were deposited on a rotating sample holder. Diffraction angles, 2θ, varied between 7° and 130° by steps of 0.04° for the first experiments, and between 7° and 70° by steps of 0.06° for the followings. *CrI* was determined from the ratio of the crystalline contribution estimated from the crystalline peaks to the total area of the diffractograms. As described in our previous work, the shape of the amorphous contribution was estimated from the diffractogram of a quasi amorphous sample (Osorio-Madrazo et al., 2010).

Transmission electron microscopy (TEM). TEM observations were performed on a Philips CM120 electron microscope operating at an accelerating voltage of 80 kV. A droplet of a dilute suspension of non-hydrolyzed or hydrolyzed chitosan particles was deposited and allowed to dry on a carbon-coated grid.

Table 2
Characteristics of products obtained in the second solid-state hydrolysis step of Ch1-D2 with 3 M HCl at room temperature (~22 °C).

Hydrolyzed chitosan	Time (h)	$M_n/10^5$ (g/mol)	DP_n	I_p	L_{110} (nm) anhydrous peak $2\theta \sim 15^\circ$	Anhydrous polymorph (%)	*CrI* (%)	Yield (%, w/w)
Second step after a first 25 h hydrolysis								
H5	25.0	1.03 ± 0.02	637 ± 1	2.22 ± 0.02	6.3	32.3	72.1 ± 0.8	91.4
H5-1	25.0 + 6.0	1.01 ± 0.03	626 ± 2	2.15 ± 0.02	5.7	38.0	73.7 ± 0.6	89.3
H5-2	25.0 + 12.3	0.99 ± 0.02	616 ± 1	1.79 ± 0.01	5.8	39.5	75.5 ± 0.6	87.8
H5-3	25.0 + 24.0	0.97 ± 0.02	599 ± 1	1.82 ± 0.02	6.0	38.0	75.9 ± 0.8	87.0
H5-4	25.0 + 49.2	0.93 ± 0.04	579 ± 3	1.88 ± 0.02	5.8	36.9	76.0 ± 0.7	85.7
Second step after a first 49 h hydrolysis								
H6	49.0	0.97 ± 0.02	602 ± 1	2.18 ± 0.02	7.4	31.9	72.8 ± 0.8	90.0
H6-1	49.0 + 6.0	0.95 ± 0.03	591 ± 2	2.21 ± 0.02	6.4	38.5	75.0 ± 0.6	88.1
H6-2	49.0 + 12.5	0.94 ± 0.02	584 ± 1	2.03 ± 0.02	6.4	40.2	77.8 ± 0.5	86.5
H6-3	49.0 + 29.8	0.92 ± 0.03	570 ± 2	2.40 ± 0.02	6.0	35.8	78.2 ± 0.8	85.3
H6-4	49.0 + 49.0	0.90 ± 0.04	559 ± 3	1.80 ± 0.01	5.8	35.5	78.0 ± 0.8	84.5

3. Results and discussion

3.1. Characterization of the crystalline structure of the starting samples

The X-ray fiber diffraction pattern of the hydrated (tendon) polymorph of chitosan was first obtained by Clark and Smith (1936) then, more recently, in a similar manner, by Okuyama, Noguchi, Miyazawa, Yui, and Ogawa (1997). An orthorhombic unit cell was proposed with the following dimensions: $a = 8.95$, $b = 16.97$ and c (fiber axis) = 10.34 Å. In this form, the molecule has a 2_1 helical symmetry, and the conformation is stabilized by O3···O5 hydrogen bonds. Eight water molecules are present in the unit cell, *i.e.* two molecules in an asymmetric unit (1 H_2O/monosaccharide).

The anhydrous polymorph, a second form, is obtained by annealing the hydrated allomorph at about 240 °C in water (Ogawa, 1991; Ogawa et al., 1984; Saito et al., 1987). It gives rise when polymer chains are broken and hydrophobic interactions favored. The corresponding diffraction pattern displays a strong (1 1 0) reflection at $2\theta \approx 15^\circ$ absent in the tendon form. Ogawa et al. (1984) proposed that this polymorph is energetically more stable due to additional inter-chain hydrogen bondings formed upon the removal of loosely bound water molecules between chains along the [0 1 0] direction in the tendon chitosan (Ogawa et al., 1984; Saito et al., 1987). Saito et al. (1987) obtained annealed samples after heating chitosan in water at 200–220 °C confirming that the relative proportion of the different polymorphs in the annealed samples depends on temperature, the origin and molecular weight (Ogawa, 1991; Ogawa et al., 1984; Saito et al., 1987). Ogawa (1991) also examined the crystallinity changes in aqueous suspensions. Okuyama et al. (1999) obtained this form by keeping a chitosan/acetic acid complex in 100% RH for several days, at room temperature. The mild conditions contributed to a well-preserved orientation and crystallinity, compared to those obtained by annealing, with a better description of the three-dimensional structure of the new allomorph (Okuyama et al., 1999). In this polymorph there is no direct interaction between successive sheets of polymer chains along the *a*-axis. Chitosan molecules have a two-fold helical symmetry and the conformation in the unit cell is stabilized by strong O3···O5 and weak O3···O6 hydrogen bonds within a repeating period of 10.43 Å.

WAXS diffraction patterns of the fully deacetylated and non-hydrolyzed samples Ch1-D2 and Ch1-D2′ exhibited the main peaks at $2\theta = 10.80^\circ$ for the $(0\,2\,0)_h$ planes and around 20°, corresponding to the contribution of two peaks at 20.16° and 21.80°, related to the reflections of the $(2\,0\,0)_h$ and $(2\,2\,0)_h$ planes. This is the characteristic structure of the hydrated chitosan crystals described by Clark and Smith (1936). The value of *CrI* for samples Ch1-D2 and Ch1-D2′ was 67 and 69%, respectively (Table 1), as calculated from X-ray diffractograms using the method proposed in our previous work (Osorio-Madrazo et al., 2010). The number-average molecular weight (M_n), the corresponding degree of polymerization (DP_n), polydispersity index (I_p) and degree of acetylation (*DA*) of these starting materials are also reported in Table 1.

3.2. Multi-steps solid-state hydrolysis of fully deacetylated chitosan with HCl at room temperature

In order to increase *CrI* and better understand the crystallinity changes during the solid-state hydrolysis, multi-steps procedures were performed on fully deacetylated samples using appropriate conditions of washing between each step. Hydrolyses were carried out with concentrated HCl aqueous solutions at room temperature, considering two different experimental conditions.

3.2.1. Role of the HCl concentration in a two-steps solid-state hydrolysis of Ch1-D2

In this first set of experiments, hydrolyzates were successively washed in HCl, aqueous ammonia then distilled water: between the hydrolysis steps, and at the end of the procedure. Finally, they were freeze-dried before characterization.

A first multi-steps hydrolysis of Ch1-D2 was performed with 3 M HCl (Table 2, and Table 2 in our previous work (Osorio-Madrazo et al., 2010) for characterized samples of the first hydrolysis step). Taking into account the natural water content of Ch1-D2 and the amount used in the hydration step, the effective HCl concentration was then of 1.53 M. For clarity, and for all cases studied in this work, we only report the concentration of added HCl, without stating the dilution.

In the first hydrolysis step, the decrease in DP_n with time was weak (Table 2 in our previous work (Osorio-Madrazo et al., 2010) and Fig. 1 (empty squares)). A monomodal molecular weight distribution was observed at all studied times and the products were recovered above 90%. Under these conditions, the macromolecular structure was almost preserved after hydrolysis. The increase in *CrI* was weak, and a plateau was reached at ~72% (Fig. 2). Therefore, the progress of the hydrolysis in the amorphous regions seemed to be limited as confirmed by the low decrease in DP_n. X-ray diffraction patterns of the hydrolyzates differed from those of the starting samples where only the peaks of the hydrated (h) polymorph were observed (Fig. 3I (0 h; 25 h)). After hydrolysis and washings, a well defined peak appeared at near $2\theta = 15^\circ$ thus revealing the presence of the anhydrous (a) polymorph. In the solid state, hydrolysis should occur preferably in the amorphous domains yielding oligomers mostly soluble and eliminated by washings, but chain ends, remaining bonded to the crystalline bundles, were also likely to crystallize in the anhydrous form (Osorio-Madrazo et al., 2010).

We estimated the contribution of each polymorph to the diffractograms with a powder diagram simulation tool, introducing the

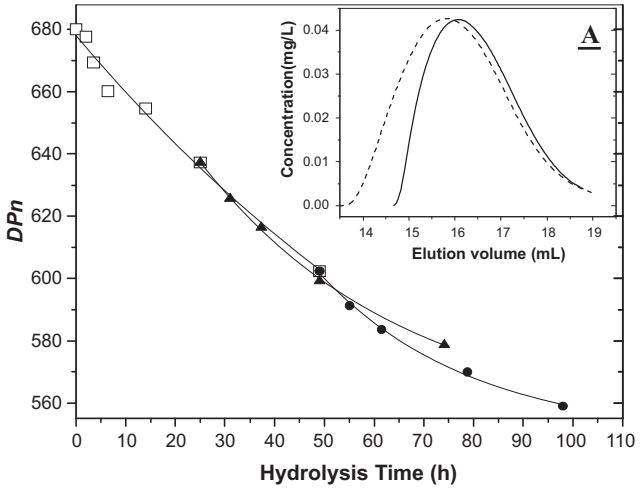

Fig. 1. Evolution of the number-average degree of polymerization (DP_n) during the multi-steps solid-state hydrolysis of Ch1-D2 with 3 M HCl at room temperature as discussed in Section 3.2.1: -□- first step including the starting points of the second hydrolysis, i.e. 2nd steps starting with the hydrolyzates produced after: -▲- 25, and -●- 49 h. Inset A: SEC/MALLS chromatograms (refractive index detector); dashed line: non-hydrolyzed reference sample Ch1-D2; solid line: Ch1-D2 after a two-steps hydrolysis (49 + 12.5 h) with 3 M HCl at room temperature ~22 °C.

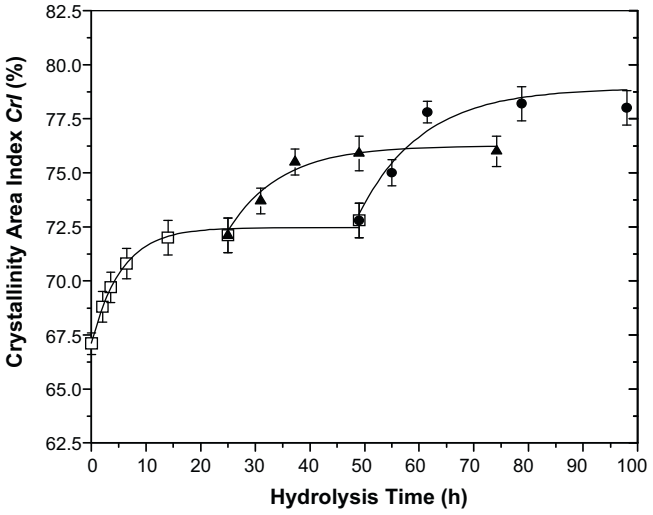

Fig. 2. *CrI* variation for Ch1-D2 during the multi-steps solid-state hydrolysis with 3 M HCl at room temperature as discussed in Section 3.2.1: -□- first step; second step starting with hydrolyzates produced after: -▲- 25, and -●- 49 h.

coordinates of atoms in the unit cell for anhydrous (Okuyama et al., 1999) and hydrated polymorphs (Okuyama et al., 1997), using the PowderCell 2.4 software by W. Kraus and G. Nolze (Federal Institute for Materials Research and Testing (BAM).). The refinement of the diffraction patterns of our hydrolyzates was carried out in the 2θ range within 8° and 27°, where the contribution of the amorphous phase is weak compared to the crystalline contribution (Fig. 3) (Osorio-Madrazo et al., 2010). The unit cell parameters were optimized for both crystalline phases, maintaining constant the relative atom coordinates (Okuyama et al., 1999, 1997). The background was set to a constant value as well as the full-width at half-maximum (FWHM) of the peaks for each allomorph. The refinement yielded the scaling factor for each phase and the corresponding fraction of the two polymorphs. The re-crystallization into the anhydrous allomorph was favored by a relatively higher molecular mobility of hydrolyzed species and conditions in favor of hydrophobic interactions (Ogawa, 1991) (in a highly acidic medium) during hydrolysis. Besides, a partial transition from the initial hydrated to the anhydrous polymorph should be taken into account after observing that the anhydrous proportion increased by ~30% with the hydrolysis whereas *CrI* only increased by ~2% (see Table 2 in our previous work (Osorio-Madrazo et al., 2010) and Fig. 2). For β-chitin, the polymorph transition from the hydrated to the anhydrous form has also been observed, by drying (Kobayashi, Kimura, Togawa, & Wada, 2010). By reducing the RH from 100 to 30%, the hydrated β-chitin crystals initially observed in the native chitin fibers from the vestimentiferan *Lamellibrachia satsuma* were converted into the anhydrous form.

The apparent widths, L_{hkl}, of anhydrous and hydrated crystals were deduced using the Scherrer equation. The FWHM of the $(1\,1\,0)_a$ and $(0\,2\,0)_h$ reflections at near $2\theta = 15°$ and 11° were used to estimate $L_{1\,1\,0}$ of the anhydrous and $L_{0\,2\,0}$ of hydrated crystals, respectively (see Table 2 in our previous work (Osorio-Madrazo et al., 2010)). These dimensions could be an indication of the equatorial development (cell parameter *c*: fiber axis) of the corresponding crystals during hydrolysis, but the fine microstructure in term of arrangement of the crystals with respect to the fiber axis will be presented in a following paper.

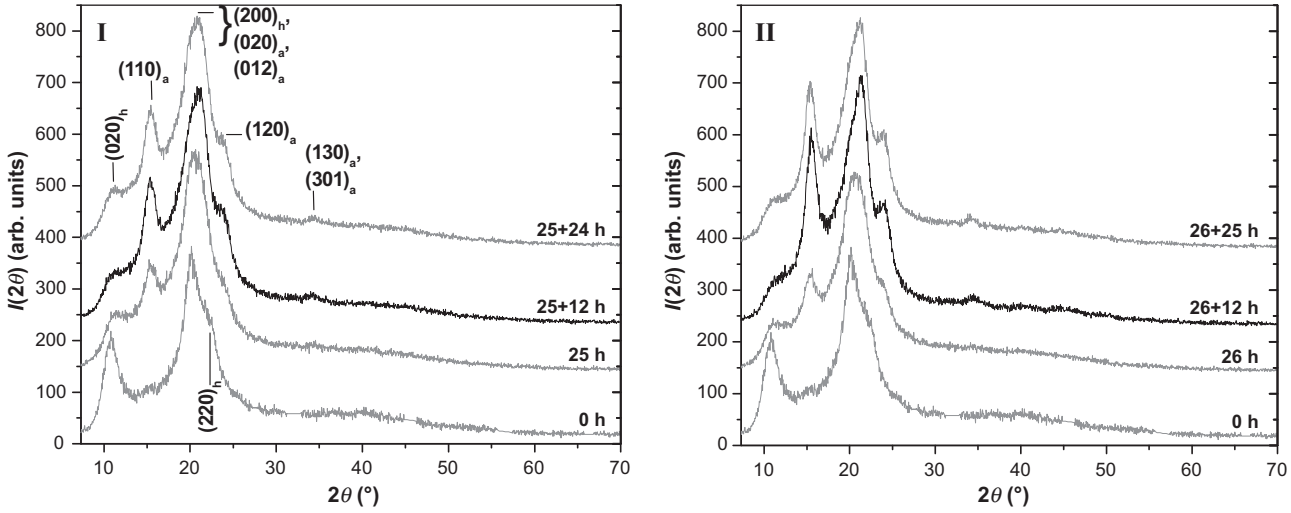

Fig. 3. WAXS diffraction patterns obtained for samples in the first (~25 h) and second step hydrolysis at different times starting with Ch1-D2 after pre-hydrolysis lasting ~25 h with: (I) 3 M HCl; and (II) 12 M HCl, at room temperature. The multi-steps hydrolyses were achieved according to the method discussed in Section 3.2.1.

To re-increase the crystallinity, we performed a second hydrolysis on products hydrolyzed during 25 or 49 h in a first step. After the first hydrolysis, they were triple washed as described above and left to stand at ambient atmosphere to allow the water evaporation up to the amount chosen for the pre-hydration. The latter added to the water present in aqueous HCl used in the next hydrolysis step yielded r_{H_2O} equal to 60 mol/mol. Then, 3 M HCl was added to start the second hydrolysis. At last, hydrolyzates were triple washed as above and freeze-dried for characterization.

During this second hydrolysis step, the decrease of M_n (or DP_n) with the hydrolysis time remained relatively moderate (below 10%) as for the first (Fig. 1), still with monomodal molecular weight distributions for all studied times. Therefore, here also, the macromolecular structure was relatively preserved, and the products recovered above 85% (Table 2).

Diffraction patterns obtained in the second step (Fig. 3I) exhibited a re-increase of *CrI* (Table 2). Fig. 2 shows the kinetics of *CrI* variation in the second step. The superimposition with that of the first reveals that the second treatment was likely to increase again *CrI*, from 72 to 76, and even to 78% for pre-hydrolyzates of 25 and 49 h, respectively. Nevertheless, in both cases, a plateau was again observed. The anhydrous polymorph proportion also re-increased appreciably from the beginning of the second step (see in Fig. 3I the increase in intensity of the peak near 15). From 32% in the pre-hydrolyzates (samples H5 and H6), it achieved 40% after 12 h of second hydrolysis (see samples H5-2 and H6-2 in Table 2 and the corresponding diffractogram of sample H5-2 in Fig. 3I (25 + 12 h)). This represents the highest proportion obtained in the second step. For longer times, it decreased to become close to 37 and 35.5% at 49 h of second hydrolysis for samples pre-hydrolyzed during 25 and 49 h, respectively. The final proportion was always over that of the first step (Fig. 3I), in spite of a decrease for long times. The apparent width $L_{1\,1\,0}$ (Table 2) of anhydrous crystals present in hydrolyzates of the second steps was similar to that obtained in the first.

The clear restart of the increase of the crystalline parameters with the second step should only be attributed to the treatments operated between the steps, especially the different washings performed before a new addition of HCl. They probably removed a part of anhydrous crystals, mainly those produced from the lowest molecular weights constituting a relatively hydrophobic barrier (see further discussion in Section 3.2.2). This allowed a new access of reagents to amorphous regions also favoring the re-crystallization of new hydrolyzed domains as anhydrous polymorph and then, a re-increase of crystallinity. At longest times, the fraction of anhydrous allomorph slightly decreased due to the preferential hydrolysis of the anhydrous allomorph probably formed at the surface of hydrated crystals (Osorio-Madrazo et al., 2010).

To increase still more the crystallinity, a second set of multi-steps experiments was operated with a higher concentration in HCl (12 M), corresponding to an effective concentration of 6.79 M. This contributed to increase both the concentration of catalyst and the hydrophobicity of the medium. Experiments were processed in conditions similar to those used with 3 M HCl. The second step was also performed with two different conditions starting with pre-hydrolyzates obtained from a first step of about 26 and 51 h. The results obtained in both cases are reported in Table 3 and Figs. 4 and 5.

DP_ns obtained after the second steps were still high (Table 3 and Fig. 4). Moreover, the molecular weight distributions remained mono-modal and percentages of collected solid product were over 80%.

CrI values were much higher than at similar times in the second step with 3 M HCl (see Fig. 6 and the comparison in Fig. 3). It increased up to 82 (sample H5-4C) and 88% (sample H6-4C) after a second hydrolysis of 50 h for a sample hydrolyzed 26 or 51 h in the first step, respectively (Fig. 5). The increase of *CrI* in these steps is

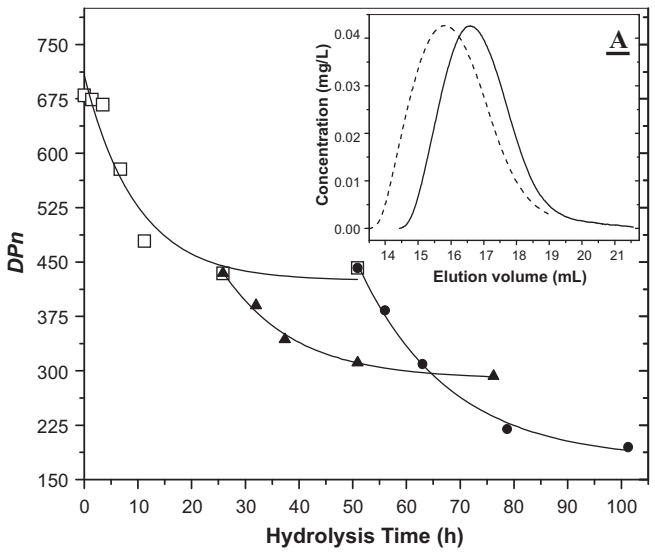

Fig. 4. Evolution of DP_n during the multi-steps solid-state hydrolysis of Ch1-D2 with 12 M HCl at room temperature as discussed in Section 3.2.1: -□- first step including the starting points of second steps for the hydrolyzate produced after: -▲- 26 and -●- 51 h.

quite high and probably yields a fraction close to 100% crystalline. Indeed, simulations of the powder diffraction diagrams by means of the atomic coordinates in the crystalline phases given by Okuyama et al. (1999, 1997) and the PowderCell software (Federal Institute for Materials Research and Testing (BAM)) explained most of the total diffraction diagrams of our samples (including both peaks and background of the scattering curves).

In these studies with 12 M HCl, we reached the highest percentages of anhydrous polymorph of this work. They were of 50 (sample H5-2C) and 60% (sample H6-2C) after the first 12 h of reaction in the second step. Fig. 6 shows the strongest scattered intensities of the anhydrous allomorph reflections for the experiment started with the sample the most hydrolyzed in the first step (51 h). Specifically, the peak of the contribution of the $(1\,3\,0)_a$ and $(3\,0\,1)_a$ reflections of the anhydrous allomorph was clearly evidenced at $2\theta \sim 34^\circ$. It was very weak for hydrolyzates obtained above. Again,

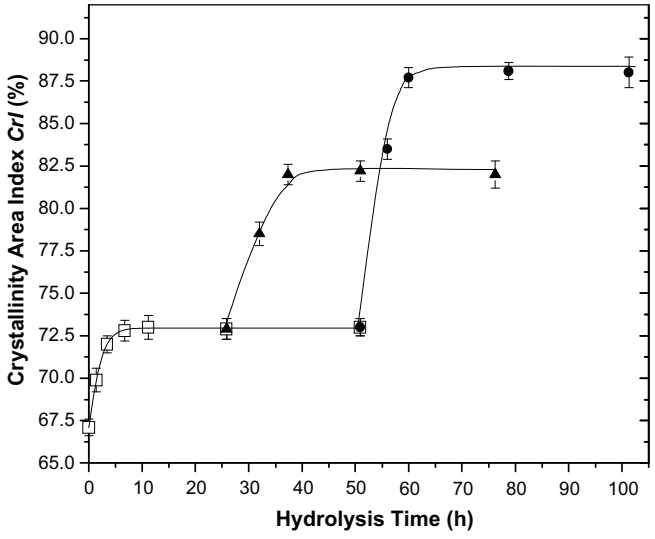

Fig. 5. Evolution of the crystallinity index (*CrI*) during the multi-steps solid-state hydrolysis of Ch1-D2 with 12 M HCl at room temperature as discussed in Section 3.2.1: -□- first step of hydrolysis including the starting points of the second steps starting for the hydrolyzate produced after: -▲- 26 and -●- 51 h.

Table 3
Characteristics of the products obtained in the second solid-state hydrolysis step of Ch1-D2 with 12 M HCl at room temperature (~22 °C).

Hydrolyzed chitosan	Time (h)	$M_n/10^5$ (g/mol)	DP_n	I_p	L_{110} (nm) anhydrous peak $2\theta \sim 15^\circ$	Anhydrous polymorph (%)	*CrI* (%)	Yield (%, w/w)
Second step after a first 26 h hydrolysis								
H5_C	25.8	0.70 ± 0.02	435 ± 1	2.55 ± 0.02	6.7	33.2	72.9 ± 0.6	88.7
H5-1C	25.8 + 6.2	0.63 ± 0.02	390 ± 1	2.06 ± 0.02	6.0	45.3	78.5 ± 0.7	86.8
H5-2C	25.8 + 11.5	0.55 ± 0.03	343 ± 2	1.77 ± 0.02	5.8	50.4	82.0 ± 0.6	84.8
H5-3C	25.8 + 25.1	0.50 ± 0.02	311 ± 1	2.76 ± 0.01	6.7	43.0	82.2 ± 0.6	83.6
H5-4C	25.8 + 50.4	0.47 ± 0.04	293 ± 3	1.39 ± 0.01	6.0	41.4	82.0 ± 0.8	82.5
Second step after a first 51 h hydrolysis								
H6_C	50.9	0.71 ± 0.02	442 ± 1	2.40 ± 0.02	5.4	32.8	73.0 ± 0.5	87.5
H6-1C	50.9 + 5.1	0.62 ± 0.03	384 ± 2	2.59 ± 0.02	6.0	53.0	83.5 ± 0.6	85.6
H6-2C	50.9 + 12.1	0.50 ± 0.02	310 ± 1	2.11 ± 0.01	6.7	59.6	87.7 ± 0.6	83.5
H6-3C	50.9 + 27.9	0.36 ± 0.03	220 ± 2	2.45 ± 0.02	6.7	54.6	88.1 ± 0.5	81.6
H6-4C	50.9 + 50.4	0.31 ± 0.04	195 ± 3	1.54 ± 0.01	6.3	51.7	88.0 ± 0.9	80.0

the concomitant increase of the anhydrous polymorph fraction up to about 60% cannot be explained only by a re-crystallization of hydrolyzed amorphous segments, but should imply a partial phase conversion of the initial hydrated to the anhydrous allomorph. This was strongly favored with the pre-hydrolyzed samples exhibiting a lower molecular weight than the non pre-hydrolyzed chitosan used in the first step. Ogawa et al. (Ogawa, 1991; Ogawa et al., 1984; Ogawa, Yui, & Miya, 1992; Saito et al., 1987) reported that the proportion of anhydrous polymorph obtained after heating aqueous suspensions of chitosan depends on the molecular weight. They obtained an X-ray diffractogram of annealed low molecular weight chitosan showing very strong peaks of anhydrous polymorph and practically no peaks of hydrated polymorph (Ogawa, 1991). In contrast, high molecular weight chitosan still showed a significant amount of hydrated polymorph due to a lower decrease in molecular weight with annealing and consequently a lower molecular mobility. It seems thus that below a critical *DP* the anhydrous form would be favored. In this work, the increase of HCl concentration favored more hydrophobic interactions thus contributing to the conversion of the hydrated phase to the anhydrous form even for high or medium molecular weights. As observed above, for long times, although *CrI* increased or became constant, the fraction of anhydrous allomorph decreased continuously with time. Nevertheless it still remained much higher (Table 3) than in the second steps with 3 M HCl (Table 2).

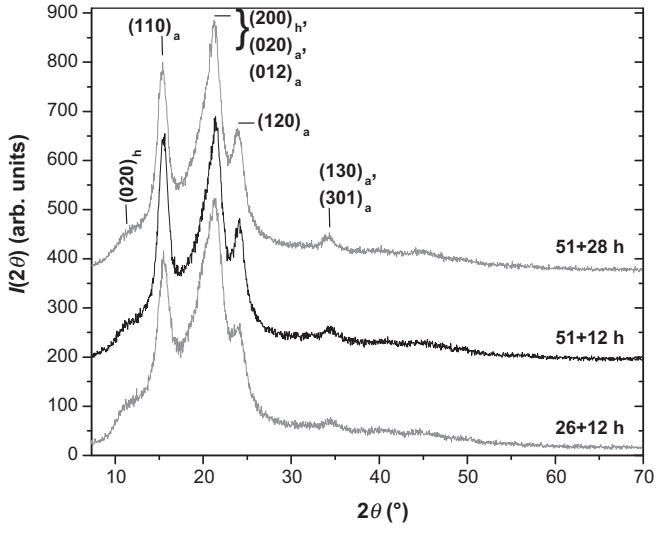

Fig. 6. WAXS diffraction patterns at different times of hydrolysis in the second-step with 12 M HCl at room temperature starting with Ch1-D2 after pre-hydrolysis during 26 or 51 h. The multi-steps hydrolyses were processed according to the method discussed in Section 3.2.1.

Transmission electron microscopy (TEM) was used to observe the microstructure of samples at different stages of hydrolysis. Fig. 7a shows a micrograph of Ch1-D2 constituted of rough and ill-defined particles, and Fig. 7b that of a dilute suspension of Ch1-D2 hydrolyzed 51 h in a first step with 12 M HCl (sample H6-C). A fibrillar network after the first hydrolysis step is clearly evidenced. Fig. 7c shows a TEM micrograph of the hydrolyzate H6-2C obtained after the second hydrolysis of H6_C during 12 h. Particles contain slender domains of different sizes which appear attached to a denser trunk of non isolated fibrils. The width of the fibrils (either tails or tie-fibrils) was measured between 60 and 155 nm with an average value of 110 ± 5 nm. The length of the fibril tails was largely heterogeneous, ranging from 0.44 to 7 μm. These dimensions lead to aspect ratios L/d (with L the length and d the diameter) as high as those of highly crystalline chitin rods (whiskers) obtained from *Riftia* tubes (L = 0.5–10 μm, d = 18 nm, L/d = 120) (Morin & Dufresne, 2002), in the range of those reported for chitin whiskers obtained from crab shells (L = 100–600 nm, d = 4–40 nm, average L/d around 16) (Gopalan Nair & Dufresne, 2003), and from squid pens (L = 50–300 nm, d = 10 nm, L/d = 15) (Paillet & Dufresne, 2001).

So far, the terminology 'whiskers' has been used for single crystalline entities with a rod-like morphology. As mentioned above, for polysaccharides like chitin, whiskers of both β- and α-polymorphs have been reported. Thus, the acid hydrolysis of vestimentiferan worms (*e.g. Riftia*, *Tevnia*) produces microfibrils where the chitin chains form a perfect mono-crystal arrangement of β-chitin of several microns length, and a width around 18 nm (Morin & Dufresne, 2002) almost preserving the original diameter of the fibrils in the organisms before hydrolysis (30–50 nm) (Gaill, Persson, Sugiyama, Vuong, & Chanzy, 1992). Whiskers of ~250 nm length and ~15 nm width obtained by hydrolysis of arthropod shell (Gopalan Nair & Dufresne, 2003) does not correspond to individual crystals but to a bundle of 2 or 3 individual α-chitin mono-crystals of no more than 3 nm in diameter (Giraud-Guille, Chanzy, & Vuong, 1990; Revol & Marchessault, 1993).

Nevertheless, our hydrolyzed particles revealed a network of substantially curved and interconnected microfibrils. This is different from the whiskers morphology, which consists of independent straight slender rods. To obtain either independent monocrystals or bundles of monocrystals, namely whiskers; one could think to a classical procedure of preparation including a boiling of a suspension of chitosan in concentrated HCl followed by a shearing, but, in our case, previous attempts only led to particles with almost a square shape, thus, with a rather low aspect ratio. Therefore, the preparation of whiskers from our particles could be instead completed with an ultrasonic treatment to process isolated slender rods. Doing so, one should pay attention to the molecular consequences as this necessarily causes chain degradations (Chen, Shyur, & Chang, 1997; Takahashi, 1997; Takahashi, Miki, &

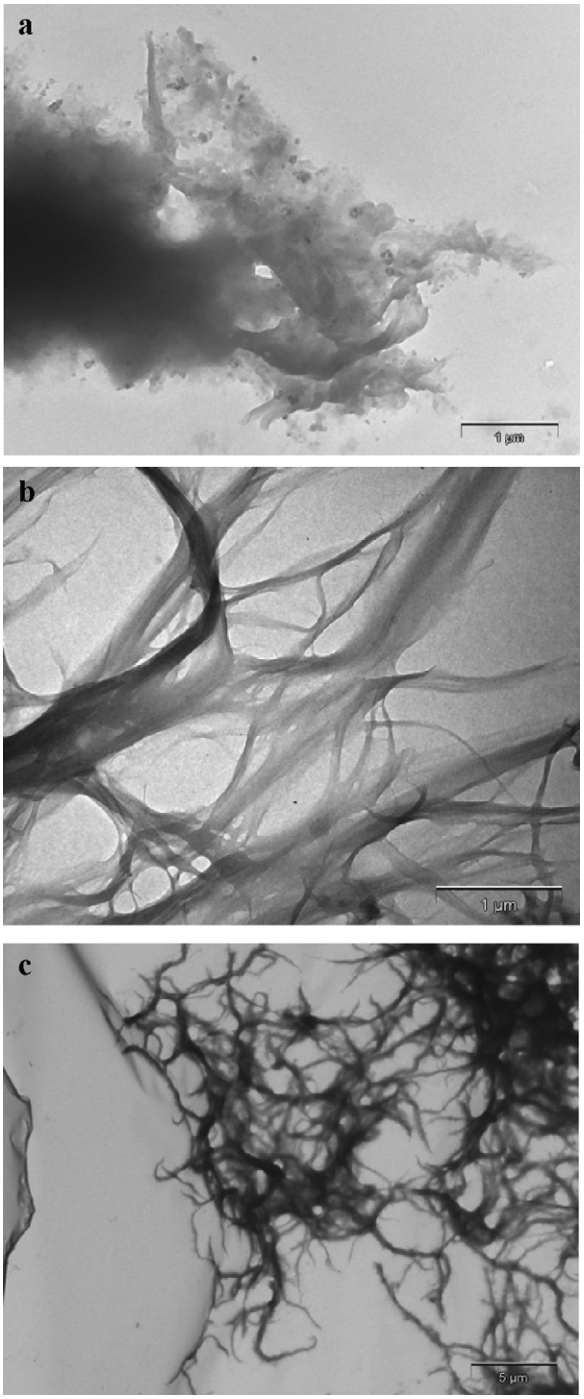

Fig. 7. Transmission electron micrographs of dilute suspensions of microcrystalline chitosan particles of: (a) flakes of raw original Ch1-D2, (b) Ch1-D2 hydrolyzed with 12 M HCl during 51 h (sample H6_C, Table 3), (c) hydrolyzate H6-2C (Table 3) obtained from the second 12 h hydrolysis of 51 h pre-hydrolyzate as discussed in Section 3.2.1 (H6-2C was the sample with the highest proportion of anhydrous polymorph (60%)).

Nagase, 1995). A further study of the microstructure of our crystalline particles, reporting on the arrangement of crystallites and amorphous domains within the microfibrils as well as about the relation between the polymer chain and fiber axes, is still lacking. This will be discussed in detail in a last paper.

To summarize, the decrease in the DP_n reduction rate during the initial stage of the reaction was more evidenced at high HCl concentration. The instantaneous reaction rate estimated from the tangent slope (dDP_n/dt) in the plot of DP_n *versus* hydrolysis time showed that after only 11 h, the rate decreased of about 65% of the global decrease (values not shown, but see the plot DP_n *versus t* in Fig. 4). This initial decrease was followed by a considerably slower but anyhow further decrease (Fig. 4), suggesting a barrier effect by species which could be the anhydrous polymorph crystals appearing after hydrolysis and isolation. This behavior is directly related to the typical physico-chemical context of the solid-state hydrolysis, and to the preserved heterogeneity of the semi-crystalline microstructure of chitosan where the crystallites act as barriers to the diffusion of hydrolysis reactants.

At the beginning of all second hydrolysis, an increase of the anhydrous polymorph proportion was observed. This suggested both a partial conversion of products of hydrolysis, and a local polymorphic transition into this allomorph. The highest fraction corresponded to the sample hydrolyzed during only 12 h in the second step, starting either from chitosan pre-hydrolyzed for about 25 or 51 h. This was found with both 3 and 12 M HCl. The barrier effect seemed to be constantly operating, associated to the formation of anhydrous crystals. After washings, such a protection was partly destroyed and amorphous regions could be again accessible for hydrolysis and re-crystallization in the anhydrous form. On the other hand, the hydrated crystals were also more accessible to the hydrophobic environment of the amorphous swollen matrix (see discussion at the end of Section 3.2.2). In the late stages of hydrolysis, some anhydrous crystals were hydrolyzed, inducing a final decrease of their proportion over 12 h in the second step. Consistently, with 12 M HCl, the anhydrous polymorph proportions obtained in the second step were much higher than with 3 M HCl in relation with a more hydrophobic medium.

3.2.2. Strategy of washing and isolation of the hydrolyzates

To better explain the role of the washings between hydrolysis steps on the increase in crystallinity, a multi-steps procedure using different conditions was performed. Therefore, hydrolyzates were only washed with concentrated (1.5 M) HCl between two successive steps, then, concentrated HCl was added (with the same hydration conditions as in the above studies) to initiate the following step. Taking into account that the highest values of *CrI* were obtained with 12 M HCl, we maintained this concentration. Nevertheless, the remaining solid after the whole multi-steps procedure was washed successively with HCl, aqueous ammonia and water, as above. The study of the first hydrolysis step by isolating the samples simply by evaporation after a triple washing (Table 4) showed that this mode of isolation (evaporation) did not play a significant role, especially as concerns the molecular weight distribution, *CrI*, and the relative proportion of both allomorphs. Regardless the difficult reproducibility when working in heterogeneous conditions, all results (Table 4 and Figs. 8 and 9) could be considered as similar to those of Table 6 reported in our previous work (Osorio-Madrazo et al., 2010) when the samples were isolated by freeze-drying.

Therefore, in this multi-steps study, the remaining solid was dried by evaporation after the whole procedure and a triple washing as above. When the only washing with 1.5 M HCl was operated between two successive steps, the initial hydrolysis rate of the second step was similar to the instantaneous rate of the first, where the second one started, and the kinetics curve was like a continuation of the first (Fig. 8).

With this single washing with 1.5 M HCl between steps, the multi-hydrolyzed samples did not exhibit a substantial re-increase of *CrI* (Fig. 9). A plateau was reached, with a relatively low value of 77% after two-hydrolysis steps. Moreover, a lag time, at the beginning of the second step curve of *CrI versus* time (Fig. 9) was noticed. In this case, the content of anhydrous polymorph after the multi-steps processes was also low. The highest value reached was 38% after the second step and 42% after the third (Table 5 and Fig. 10). Again, for longer times, it decreased slightly with time (Fig. 10).

Table 4
Characteristics of Ch1-D2′ hydrolyzates and hydrolyzed chitosans obtained by solid-state hydrolysis of Ch1-D2′ with 12 M HCl at room temperature (~22 °C) and drying by water evaporation.

Hydrolyzed and starting chitosan	Time (h)	$M_n/10^5$ (g/mol)	DP_n	I_p	L_{020} (nm) hydrated peak $2\theta \sim 11°$	L_{110} (nm) anhydrous peak $2\theta \sim 15°$	Anhydrous allomorph (%)	*CrI* (%)	Yield (%, w/w)
Ch1-D2′	0	1.16 ± 0.03	720 ± 2	1.55 ± 0.01	4.3	~0	~0	68.5 ± 0.6	–
H1_Ev	1.0	1.15 ± 0.02	713 ± 1	2.01 ± 0.01	3.5	6.0	29.0	70.5 ± 0.6	94.0
H2_Ev	3.0	1.13 ± 0.02	700 ± 1	2.09 ± 0.02	3.5	9.5	30.8	72.4 ± 0.8	93.2
H3_Ev	7.0	0.99 ± 0.03	614 ± 2	2.69 ± 0.02	n.d.	6.1	32.2	73.6 ± 0.8	92.2
H4_Ev	15.3	0.83 ± 0.02	515 ± 1	2.39 ± 0.01	n.d.	5.8	32.2	74.0 ± 0.9	90.5
H5_Ev	24.0	0.75 ± 0.03	463 ± 2	2.23 ± 0.01	n.d.	5.5	32.1	73.9 ± 0.8	89.5

n.d.: not determined (difficult).

Table 5
Characteristics of the products obtained in the multi-steps solid-state hydrolysis of Ch1-D2′ with 12 M HCl at room temperature (~22 °C) and drying by water evaporation.

Hydrolyzed chitosan	Time (h)	$M_n/10^5$ (g/mol)	DP_n	I_p	L_{110} (nm) anhydrous peak $2\theta \sim 15°$	Anhydrous polymorph (%)	*CrI* (%)	Yield (%, w/w)
Second step after a first 7 h hydrolysis								
H3_Ev	7.0	0.99 ± 0.03	614 ± 2	2.69 + 0.02	6.1	32.2	73.6 ± 0.8	92.2
H3Ev-1	7.0 + 2.5	0.87 ± 0.03	540 ± 2	1.92 ± 0.01	6.1	32.2	73.6 ± 0.9	91.5
H3Ev-2	7.0 + 4.5	0.86 ± 0.02	534 ± 1	1.90 ± 0.01	6.4	34.0	74.5 ± 0.7	91.0
H3Ev-3	7.0 + 17.0	0.69 ± 0.03	427 ± 2	2.00 ± 0.01	6.4	38.1	77.1 ± 0.6	89.5
H3Ev-4	7.0 + 27.0	0.60 ± 0.04	374 ± 3	2.05 ± 0.01	6.7	36.5	77.0 ± 0.6	88.6
Third step after a first 7 h and a second 4 h hydrolysis steps								
H3Ev2-1	7 + 4.5 + 12.5	0.65 ± 0.03	403 ± 2	1.72 ± 0.01	7.2	39.0	78.6 ± 0.6	90.4
H3Ev2-2	7 + 4.5 + 22.3	0.47 ± 0.02	294 ± 1	2.58 ± 0.02	6.1	41.5	78.6 ± 0.6	89.0
H3Ev2-3	7 + 4.5 + 27.0	0.38 ± 0.04	237 ± 3	2.06 ± 0.01	6.4	40.6	78.4 ± 0.5	87.5
H3Ev2-4	7 + 4.5 + 57.8	0.25 ± 0.03	152 ± 2	2.68 ± 0.02	6.4	39.5	78.4 ± 0.6	85.5
Other two-steps hydrolyzate								
HEv_12h_12h	12.0 + 12.0	0.69 ± 0.03	430 ± 2	1.90 ± 0.01	6.0	39.5	77.5 ± 0.6	89.5

These results were different from those obtained when successive acidic–basic washings were operated between steps, where an abrupt increase in the proportion of anhydrous polymorph and the crystallinity was observed.

To complete this study, a single 24 h hydrolysis was compared with two successive 12 h steps (see Fig. 9), and a 7 + 4.5 + 12.5 h three-steps hydrolysis was compared to a single 24 h step. Here also, the kinetics plot of DP_n appeared as a continuous evolution of the first and second steps, respectively (Fig. 8 and Table 5), with a mono-modal molecular weight distribution. The percentage of anhydrous polymorph was only slightly higher than for a one 24 h step. If the above third step was prolonged up to almost 60 h, *CrI* remained practically the same at near 78% (Fig. 9), but somewhat higher than above after the second step.

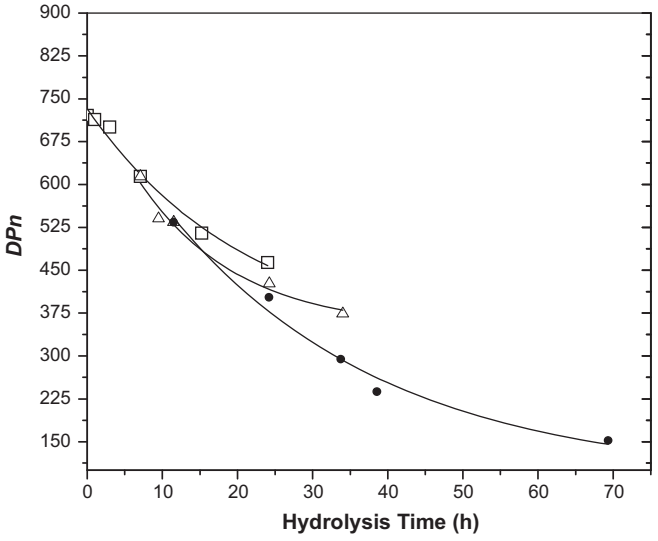

Fig. 8. Decrease of DP_n during the multi-steps solid-state hydrolysis of Ch1-D2 with 12 M HCl at room temperature: -□- first step of hydrolysis; -△- second step starting with the hydrolyzate produced after a first step lasting 7 h and after washing between the two steps only in HCl, -●- third step after: a first hydrolysis lasting 7 h, washing only in HCl, second hydrolysis lasting 4.5 h, washing only in HCl. After one-, two-, or three-steps hydrolysis, the solid hydrolyzate to be characterized was washed in HCl, then in ammonia, distilled water, and dried by water evaporation.

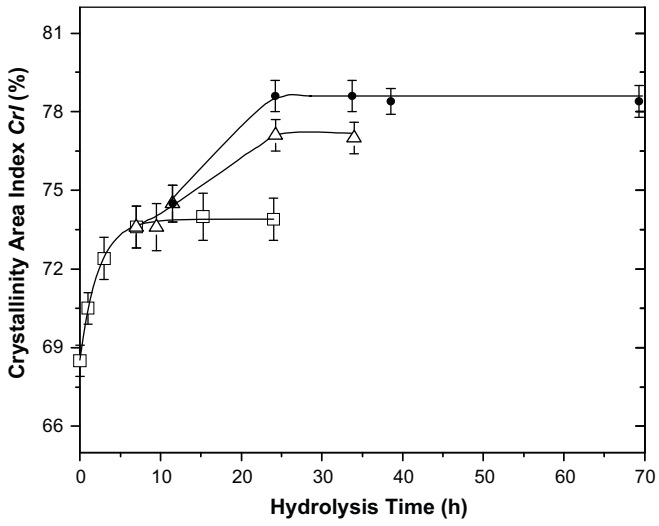

Fig. 9. Evolution of *CrI* during the multi-steps solid-state hydrolysis of Ch1-D2 with 12 M HCl at room temperature: -□- first step of hydrolysis; -△- second step starting with the hydrolyzate produced after a first step lasting 7 h and after washing between the two steps only in HCl, -●- third step after: a first hydrolysis lasting 7 h, washing only in HCl, second hydrolysis lasting 4.5 h, washing only in HCl. After one-, two-, or three-steps hydrolysis, the solid hydrolyzate to be characterized was washed in HCl, then in ammonia, distilled water, and dried by water evaporation.

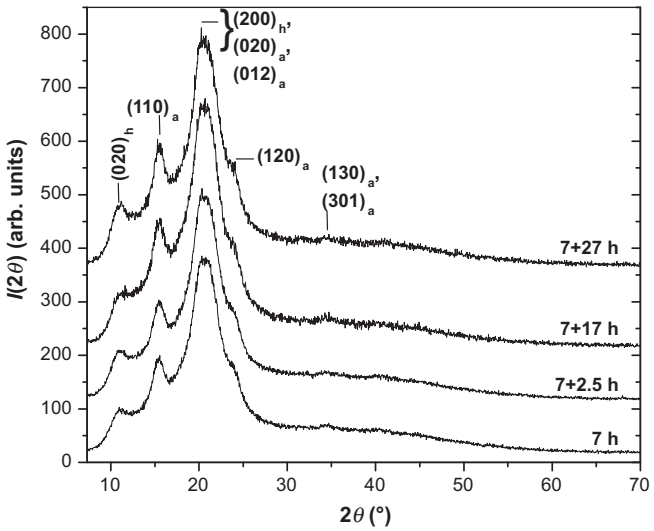

Fig. 10. WAXS diffraction patterns of hydrolyzates obtained at different times of hydrolysis in the first (7 h) and second step with 12 M HCl at room temperature (starting with Ch1-D2′ after pre-hydrolysis lasting 7 h and washing between the two steps only in HCl). After one- or two-steps hydrolysis, the solid to be characterized was washed in HCl, then, in ammonia, distilled water, and dried by water evaporation.

It becomes clear that a key parameter to obtain high *CrI* values and favor the formation of anhydrous polymorph was to operate successive acidic and alkaline washings between the different hydrolysis steps. The first with HCl allowed the elimination of low molecular weight oligomers, especially those of $DP < 15$, soluble and partially hydrolyzed in this medium. They also constitute the anhydrous polymorph crystals operating as a barrier inhibiting the progress of the hydrolysis through the rest of the amorphous phase. The second with 1 M ammonia, in addition to complete the elimination of small oligomers ($DP < 6$) (Belamie, Domard, & Giraud-Guille, 1997) contributed to convert the protoned form of chitosan into free amine. During this change, a very partial hydration and dissolution of polymer chains was operated, in relation with the solubility region of a fully deacetylated chitosan, between

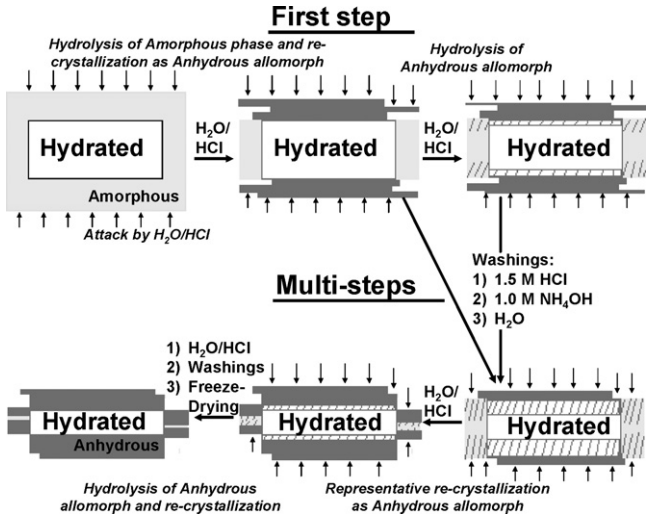

Fig. 11. Scheme proposed for crystallization changes involving hydrated, anhydrous and amorphous phases during the solid-state acid hydrolysis of chitosan. Fillers represent: *white:* hydrated crystals; *gray:* amorphous phase, *dark gray:* anhydrous crystals; and *dashed:* intermediary stages of polymorphic transition. The external arrows represent the attack by the concentrated aqueous HCl (used as hydrolysis reagent) into the chitosan microstructure.

pH 2 and 5 (Domard, 1997; Sorlier, 2002) and complete the dissolution of low *DP* oligomers ($DP < 15$) trapped in the crystallites (anhydrous). The third washing with water induced the elimination of both NH_4Cl formed during the neutralization and the excess of ammonia. Finally, the hydrolysis restarted in the following step adding HCl and therefore a reverse conversion of the free amine form to the protoned one, again allowing a local hydration and dissolution of polymer chains. This double conversion from protoned to free amine and back to the protonated form of chitosan, is necessarily responsible of a partial destruction of hydrogen bonds inside the network of chitosan chains. Besides, the exothermic character of the reactions carried out by the successive washings is likely to bring a sufficient energy to favor this effect. Finally, it induced a better accessibility to the structure and therefore, an important re-increase in crystallinity due to: (i) a swelling and reorganization of the amorphous phase, (ii) a partial dissolution of the crystalline phase, and (iii) a partial elimination of the barrier effect of the anhydrous crystals.

When hydrolyzates are only washed with 1.5 M HCl, the double neutralization–protonation conversion cannot operate and this only contributes to eliminate low molecular weight oligomers. Therefore, this induces a very limited hydrolysis of a small amount of amorphous domains after re-hydration, explaining a slight increase, in this case, of both the crystallinity and the fraction of anhydrous crystals. Besides, the barrier effect due to anhydrous crystals remained present after this single washing step and protected hydrated crystals and amorphous regions.

To conclude, the latter study reveals that the number of steps does not alone influence crystallization changes. It is indeed necessary to consider the beneficial effects of appropriate washings between two hydrolyses steps.

The second typical behavior observed in all our kinetics studies was that *CrI* always achieved a plateau in spite of the continuous decrease of DP_n and the slight decrease in the fraction of anhydrous polymorph. The important initial increase of anhydrous crystals that should form essentially at the surface and the surrounding of the hydrated crystallites can explain the plateau. They operated a barrier role regarding amorphous parts, and protected the hydrated crystals. This was related to a weak accessibility of the material to hydrolysis reagents resulting in an equilibrium between the hydrolysis of the anhydrous crystals at the surface of the material, and the re-crystallization in highly hydrophobic conditions of mobile species hydrolyzed in the amorphous phase. This would explain the continuous decrease of the anhydrous fraction although a plateau of *CrI* was achieved. To summarize, Fig. 11 shows a modeling scheme of crystallization changes occurring during the multi-steps hydrolysis.

4. Conclusions

The multi-steps acid hydrolysis of chitosan in the solid state, in mild conditions and in conjunction with an appropriate choice of washings between each step, appeared as an interesting process to considerably increase *CrI* and consequently produce highly crystalline microfibrils even preserving the macromolecular structure. As the hydrolysis proceeds, the crystallinity increases, mainly due to the removal of amorphous regions and the formation of crystals of anhydrous allomorph. Our results suggested that the structure became gradually more resistant to further hydrolysis as the reaction works.

Crystals of anhydrous polymorph, appeared only after hydrolysis and isolation, hindered progressively the accessibility of reagents to the remaining amorphous domains and the hydrated allomorph. This is the main explanation of the plateau observed in the *CrI* variation. The anhydrous allomorph can be

formed by re-crystallization, in highly hydrophobic conditions, of hydrolyzed polymer chains (of lower molecular weight) from amorphous regions, or from a partial conversion of the hydrated allomorph. Washings with concentrated HCl, then, concentrated ammonia and finally distilled water, were likely to destroy oligomer crystals of anhydrous polymorph so that amorphous domains became again accessible to hydrolysis in the following step. These successive washings favored the double conversion protonated/free amine/protonated form of chitosan, responsible, due to changes in pH, of a local hydration/dissolution and then, the re-crystallization of polymer chains coming from the amorphous and crystalline phases. The new hydrolyzed regions with a molecular weight appreciably lower could re-crystallize as anhydrous polymorph, and this, combined with the conversion of the hydrated to the anhydrous allomorph mentioned above, increased abruptly the proportion of this polymorph and *CrI* in the further step. With higher HCl concentration (12 M), higher *CrI* values were observed and higher anhydrous polymorph proportions were produced, in relation with more favored hydrophobic interactions.

The detailed microstructure in terms of morphology related to the molecular chain organization and crystallinity of the chitosan particles during the hydrolysis in the solid state will be studied in a last paper.

Acknowledgments

Authors thank the EC α2 Programme "Polylife" (Project II-0259-FA-FDC) for financial support; R. Vera for the experiments carried out at the *Centre de Diffractométrie Henri Longchambon* at the *Université Claude Bernard Lyon 1* (http://cdalpha.univ-lyon1.fr/); P. Alcouffe for electron microscopy observations carried out at the *Centre de Technologie des Microstructures* at the Université Claude Bernard Lyon 1; and A. Crepet for their technical assistance.

References

Angles, M. N., & Dufresne, A. (2001). Plasticized starch/tunicin whiskers nanocomposite materials. 2. Mechanical behavior. *Macromolecules*, *34*(9), 2921–2931.

Belamie, E., Domard, A., & Giraud-Guille, M. M. (1997). Study of the solid-state hydrolysis of chitosan in presence of HCl. *Journal of Polymer Science Part A: Polymer Chemistry*, *35*(15), 3181–3191.

Chen, R. H., Shyur, J. S., & Chang, J. R. (1997). Effects of ultrasonic-heating and heating only on changes of intrinsic viscosity, degree of deacetylation, and maximum melting point temperature of treated chitosan in acetic acid solution containing 4 M urea. In A. Domard, G. A. F. Roberts, & K. M. Varum (Eds.), *Advances in chitin science* (pp. 437–444). Lyon: Jacques André.

Clark, G. L., & Smith, A. F. (1936). X-ray diffraction studies of chitin, chitosan, and derivatives. *Journal of Physical Chemistry*, *40*(7), 863–879.

Domard, A. (1997). Chitosan interactions. In A. Domard, G. A. F. Roberts, & K. M. Varum (Eds.), *Advances in chitin science (II)* (pp. 410–420). Lyon: Jacque André.

Dubief, D., Samain, E., & Dufresne, A. (1999). Polysaccharide microcrystals reinforced amorphous poly(β-hydroxyoctanoate) nanocomposite materials. *Macromolecules*, *32*(18), 5765–5771.

Federal Institute for Materials Research and Testing (BAM) in Unter den Eichen 87, D-12205 Berlin. Available from http://www.ccp14.ac.uk/ccp/web-mirrors/powdcell/a_v/v_1/powder/e_cell.html.

Gaill, F., Persson, J., Sugiyama, J., Vuong, R., & Chanzy, H. (1992). The chitin system in the tubes of deep sea hydrothermal vent worms. *Journal of Structural Biology*, *109*(2), 116–128.

Giraud-Guille, M.-M., Chanzy, H., & Vuong, R. (1990). Chitin crystals in arthropod cuticles revealed by diffraction contrast transmission electron microscopy. *Journal of Structural Biology*, *103*(3), 232–240.

Gopalan Nair, K., & Dufresne, A. (2003). Crab shell chitin whisker reinforced natural rubber nanocomposites. 1. Processing and swelling behavior. *Biomacromolecules*, *4*(3), 657–665.

Kobayashi, K., Kimura, S., Togawa, E., & Wada, M. (2010). Crystal transition between hydrate and anhydrous [beta]-chitin monitored by synchrotron X-ray fiber diffraction. *Carbohydrate Polymers*, *79*(4), 882–889.

Lamarque, G., Cretenet, M., Viton, C., & Domard, A. (2005). New route of deacetylation of chitins by means of freeze-pump out-thaw cycles. *Biomacromolecules*, *6*(3), 1380–1388.

Mathew, A. P., & Dufresne, A. (2002). Morphological investigation of nanocomposites from sorbitol plasticized starch and tunicin whiskers. *Biomacromolecules*, *3*(3), 609–617.

Morin, A., & Dufresne, A. (2002). Nanocomposites of chitin whiskers from Riftia tubes and poly(caprolactone). *Macromolecules*, *35*(6), 2190–2199.

Ogawa, K. (1991). Effect of heating an aqueous suspension of chitosan on the crystallinity and polymorphs. *Agricultural and Biological Chemistry*, *55*(9), 2375–2379.

Ogawa, K., Hirano, S., Miyanishi, T., Yui, T., & Watanabe, T. (1984). A new polymorph of chitosan. *Macromolecules*, *17*(4), 973–975.

Ogawa, K., Yui, T., & Miya, M. (1992). Dependence on the preparation procedure of the polymorphism and crystallinity of chitosan membranes. *Bioscience, Biotechnology, and Biochemistry*, *56*(6), 858–862.

Okuyama, K., Noguchi, K., Hanafusa, Y., Osawa, K., & Ogawa, K. (1999). Structural study of anhydrous tendon chitosan obtained via chitosan/acetic acid complex. *International Journal of Biological Macromolecules*, *26*(4), 285–293.

Okuyama, K., Noguchi, K., Miyazawa, T., Yui, T., & Ogawa, K. (1997). Molecular and crystal structure of hydrated chitosan. *Macromolecules*, *30*(19), 5849–5855.

Osorio-Madrazo, A., David, L., Trombotto, S. P., Lucas, J.-M., Peniche-Covas, C., & Domard, A. (2010). Kinetics study of the solid-state acid hydrolysis of chitosan: Evolution of the crystallinity and macromolecular structure. *Biomacromolecules*, *11*(5), 1376–1386.

Paillet, M., & Dufresne, A. (2001). Chitin whisker reinforced thermoplastic nanocomposites. *Macromolecules*, *34*(19), 6527–6530.

Revol, J. F., & Marchessault, R. H. (1993). In vitro chiral nematic ordering of chitin crystallites. *International Journal of Biological Macromolecules*, *15*(6), 329–335.

Saito, H., Tabeta, R., & Ogawa, K. (1987). High-resolution solid-state carbon-13 NMR study of chitosan and its salts with acids: Conformational characterization of polymorphs and helical structures as viewed from the conformation-dependent carbon-13 chemical shifts. *Macromolecules*, *20*(10), 2424–2430.

Schatz, C., Viton, C., Delair, T., Pichot, C., & Domard, A. (2003). Typical physicochemical behaviors of chitosan in aqueous solution. *Biomacromolecules*, *4*(3), 641–648.

Sorlier, P. (2002). Etude physico-chimique de solutions de chitosane et relation avec ses propriétés antigéniques. Lyon: Thèse de Doctorat. Université Claude Bernard Lyon 1.

Sorlier, P., Viton, C., & Domard, A. (2002). Relation between solution properties and degree of acetylation of chitosan. Role of aging. *Biomacromolecules*, *3*, 1336–1342.

Takahashi, Y. (1997). Effect of sonication on the acid degradation of chitin and chitosan. In A. Domard, G. A. F. Roberts, & K. M. Varum (Eds.), *Advances in chitin science* (pp. 372–377). Lyon: Jacques André.

Takahashi, Y., Miki, F., & Nagase, K. (1995). Effect of sonolysis on acid degradation of chitin to form oligosaccharides. *Bulletin of the Chemical Society of Japan*, *68*, 1851–1857.

Varum, K. M., Ottoy, M. H., & Smidsrod, O. (1994). Water-solubility of partially N-acetylated chitosans as a function of pH: Effect of chemical composition and depolymerisation. *Carbohydrate Polymers*, *25*, 65–70.

Yokota, H. (1986). The selective uniplanar orientation phenomenon in chitosan sheets derived from microfibrillated chitosan. *Journal of Polymer Science Part C: Polymer Letters*, *24*(8), 423–425.